

# Magnetic excitations in $\{\text{Mo}_{72}\text{Fe}_{30}\}$

V. O. Garlea,<sup>1,\*</sup> S. E. Nagler,<sup>2</sup> J. L. Zarestky,<sup>1</sup> C. Stassis,<sup>1</sup> D. Vaknin,<sup>1</sup> P. Kögerler,<sup>1</sup> D. F. McMorrow,<sup>3,4</sup> C. Niedermayer,<sup>5</sup> D. A. Tennant,<sup>6</sup> B. Lake,<sup>7,1</sup> Y. Qiu,<sup>8</sup> M. Exler,<sup>9</sup> J. Schnack,<sup>9</sup> and M. Luban<sup>1</sup>

<sup>1</sup>Ames Laboratory, Department of Physics and Astronomy, Iowa State University, Ames, IA, 50011, USA

<sup>2</sup>Oak Ridge National Laboratory, Oak Ridge, TN 37831 USA

<sup>3</sup>Risø National Laboratory, DK-4000, Roskilde, Denmark

<sup>4</sup>Department of Physics and Astronomy, University College London, UK

<sup>5</sup>Laboratory for Neutron Scattering ETHZ & PSI, CH-5232 Villigen PSI, Switzerland

<sup>6</sup>School of Physics and Astronomy, University of St Andrews, St Andrews, FIFE KY16 9SS, Scotland, UK

<sup>7</sup>Clarendon Laboratory, University of Oxford, Parks Road, Oxford OX1 3PU, UK

<sup>8</sup>NIST Center for Neutron Research, Gaithersburg, MD & U. Maryland, College Park, MD, USA

<sup>9</sup>Universität Osnabrück, Fachbereich Physik - D-49069 Osnabrück, Germany

(Dated: May 4, 2005)

We report cold-neutron inelastic neutron scattering measurements on deuterated samples of the giant polyoxomolybdate magnetic molecule  $\{\text{Mo}_{72}\text{Fe}_{30}\}$ . The 30  $s = 5/2$   $\text{Fe}^{3+}$  ions occupy the vertices of an icosidodecahedron, and interact via antiferromagnetic nearest neighbor coupling. The measurements reveal a band of magnetic excitations near  $E \approx 0.6$  meV. The spectrum broadens and shifts to lower energy as the temperature is increased, and also is strongly affected by magnetic fields. The results can be interpreted within the context of an effective three-sublattice spin Hamiltonian.

PACS numbers: 75.25.+z, 75.50.Ee, 75.75.+a, 78.70.Nx

Magnetic molecules are ideal prototypical systems for the study of fundamental problems in magnetism on the nanoscale level [1]. As a result, their properties have been the subject of many theoretical and experimental investigations [2, 3, 4, 5, 6, 7, 8, 9, 10, 11, 12]. Of paramount importance is the determination of the magnetic excitation spectrum. However, for a molecule with  $N$  magnetic ions of spin  $s$  the calculation of the  $(2s+1)^N$  eigenstates and their energies quickly becomes impractical for increasing  $N$  and  $s$ . Neutron scattering is the most effective and direct technique for determining the magnetic energy levels, and there have been studies of excitations in several magnetic molecules containing up to 12 spins [2, 3, 4, 5, 6, 7].

In this Letter we report cold-neutron inelastic scattering results obtained on one of the largest magnetic molecules yet synthesized: the polyoxomolybdate cluster  $\{\text{Mo}_{72}\text{Fe}_{30}\}$ . The crystallographic structure is described by the space group  $R\bar{3}$  with the lattice constants:  $a \approx 55.13$  Å, and  $c \approx 60.19$  Å [9]. The molecule contains 30  $\text{Fe}^{3+}$  ions ( $s = 5/2$ ) occupying the vertices of an icosidodecahedron. The magnetic ions are interlinked by  $\text{Mo}_6\text{O}_{21}$  fragments acting as super-exchange pathways, resulting in nearest neighbor antiferromagnetic exchange  $J\vec{S}_i \cdot \vec{S}_j$  and a singlet spin ground state. As the icosidodecahedron consists of 20 corner-sharing triangles circumscribing 12 pentagons the spins are frustrated and show properties similar to the antiferromagnetic Kagomé lattice [13]. For  $s = 5/2$  it is reasonable to consider classical spin vectors as a starting point [8], leading to a picture at  $T = 0$  of three sublattices of 10 parallel spins each, with orientations defined by coplanar vectors offset by  $120^\circ$  angles. As discussed below, many features of the observed scattering can be interpreted in the context of

a solvable three-sublattice effective Hamiltonian substituted for the intractable Heisenberg Hamiltonian [8, 10].

Most of the neutron scattering experiments were performed on deuterated samples to minimize the attenuation and incoherent scattering from the hydrogen atoms. Characterization of the deuterated samples by infrared and Raman spectroscopy and X-ray diffraction confirmed that their properties were consistent with those of non-deuterated samples studied earlier [9].

The neutron measurements used polycrystalline samples of approximately 10 g sealed in copper holders under He atmosphere. Preliminary characterization by powder diffraction was performed at the HB1A instrument at HFIR. Upon cooling from room temperature the diffraction patterns in both deuterated and non-deuterated samples exhibited a remarkable increase in the background over the entire measured range of scattering angle. The presence of this scattering at large wavevectors is a clear indication that it is not magnetic in origin. It can be understood as arising from quenched static structural disorder, and is manifested as a very large zero energy peak in the inelastic scattering spectra. It presents a significant experimental challenge, and prevents a clean observation of low energy magnetic scattering.

The inelastic neutron spectra were collected at low temperatures using three different spectrometers: RITA2 at PSI, DCS at NIST, OSIRIS at ISIS. The data presented here were obtained at OSIRIS using a fixed final neutron energy  $E_f = 1.845$  meV. The results obtained with DCS and RITA2 are consistent with those of OSIRIS. A complete description of all of the results will be presented elsewhere [14].

Typical data obtained are shown in Fig. 1. The scans plotted in all figures are integrated over the range  $Q =$

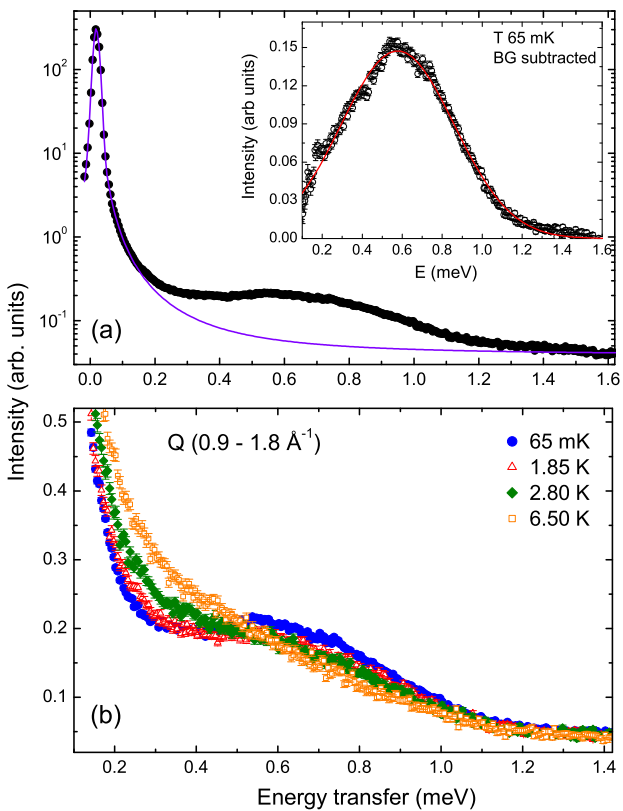


FIG. 1: (a) Inelastic neutron scattering spectrum at a nominal temperature of 65 mK. The intensity axis is on a logarithmic scale. The solid line shows a best estimate of the non-magnetic background (see text). Inset: The background subtracted scattering. (b) Raw data for several different temperatures plotted on a linear scale.

0.9 to  $1.8 \text{ \AA}^{-1}$ . Positive energies correspond to neutron energy loss. The upper panel (Fig. 1(a)) shows a semi-log plot of the spectrum at the base temperature, nominally  $T = 65 \text{ mK}$ . The large elastic peak has a FWHM of  $0.021(1) \text{ meV}$  consistent with the instrumental energy resolution. A much broader peak is visible as a shoulder in the plot. The lower panel (Fig. 1(b)) shows the scattering on a linear scale at four different temperatures ranging up to  $6.5 \text{ K}$ . At base temperature a clear peak is evident near an energy transfer of  $0.6 \text{ meV}$ . As the temperature is raised this peak weakens, and there is a notable increase in the intensity of the scattering at low energies. This behavior of the intensity is expected if the peak at  $0.6 \text{ meV}$  is due to a magnetic transition from the ground state. The temperature-enhanced low energy signal could in principle arise from lattice vibrations or from magnetic scattering, and differentiating between these possibilities requires careful analysis.

Cooling powders to mK temperatures is known to be extremely difficult, and since the temperature is measured external to the sample it is desirable to have an

internal consistency check. This can be accomplished in principle by checking the detailed balance condition, but ambiguities in the scattering background, limited data for neutron energy gain, and a resolution dependent on the energy transfer limit the precision that can be achieved. Going through this exercise suggests that the nominal sample temperatures at  $1.8 \text{ K}$  and above are probably reliable, but the base temperature to which the powder is actually cooled is less certain. The evolution of the scattering shows that it is clearly well below  $1.8 \text{ K}$  but it is likely warmer than the nominal value  $65 \text{ mK}$ . However, our data analysis does not depend on the precise value of the base temperature.

To extract more quantitative information the base temperature scattering was fit to a simple model. It was assumed that the instrumental resolution at the elastic position can be described by the sum of two co-centered peaks: a dominant Gaussian and a Lorentzian with the latter accounting for the extended tails. The nonmagnetic background scattering is taken as the sum of an elastic term proportional to the resolution function plus an energy independent constant. The magnetic scattering was assumed to be represented by a single peak, with a Gaussian found to provide a better fit than a Lorentzian. Least squares fitting of this simple model to the data was carried out initially using the entire data set. Alternatively, the analysis was repeated by determining the model background alone by fitting to the data excluding a range in the vicinity of the inelastic peak. Subsequently a single magnetic peak was fitted to the data with the above determined background subtracted. The results were found to be independent of the size of the excluded range and consistent with the fit over the whole range. The solid curve in Fig. 1(a) illustrates the background, and the inset shows the background subtracted data fit to a single Gaussian with peak position  $0.56(1) \text{ meV}$  and FWHM  $0.66(1) \text{ meV}$ . The numbers in parentheses are the estimated uncertainties in the last digit, and account for both fitting errors and systematic effects arising from different background estimations. As seen in the inset to Fig. 1(a) the overall distribution is modeled well by a single peak, however the data shows additional structure, including one or more shoulders on the low energy side. The observed energy width of the shoulders and the overall distribution are intrinsic since the resolution is roughly FWHM  $0.02 \text{ meV}$ . The signal for energy transfers greater than  $0.2 \text{ meV}$  is independent of the assumptions used in determining the background.

Further analysis was carried out to gain more insight into the temperature dependence of the scattering. A thorough attempt was made to fit the data for energy transfers less than  $0.5 \text{ meV}$  and temperatures up to  $6.5 \text{ K}$  to models of both single and multiple phonon scattering from solids or fluids [15]. This attempt was unsuccessful. Subsequently, the data was examined in a model-independent fashion, integrating the energy cuts

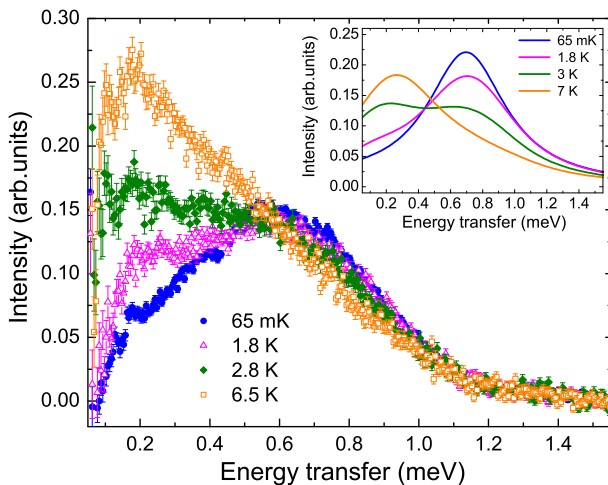


FIG. 2: Temperature dependence of the inelastic neutron scattering, plotted with the nonmagnetic background subtracted. Inset: Theoretical scattering for several temperatures, calculated using the quantum rotational band model with simplifying assumptions (see text).

over different wavevector ranges varying from  $Q_L = 1.0 - 1.2 \text{ \AA}^{-1}$  to  $Q_U = 1.6 - 1.8 \text{ \AA}^{-1}$ . It was verified that for all temperatures up to 6.5 K there is no  $Q$  dependence in the scattering to within the sensitivity of the measurement. This is a significant result since the intensity for single phonon scattering is expected to increase proportional to  $Q^2$ , and that of multiphonon scattering should increase even more rapidly with  $Q$  [15]. The intensity of phonon scattering in the range  $Q_U$  should be stronger by a factor of 2.5 or more than that in  $Q_L$ , contrary to the experimental observation. It can be concluded that phonon scattering is insignificant over the wavevector and temperature range of the data considered here.

Given this result, it is reasonable to assume that the nonmagnetic background is temperature independent. The background subtracted scattering for several temperatures up to 6.5 K is shown in Fig. 2. With the uncertainties in temperature and instrumental resolution there may be some amount of magnetic scattering included as background at low energy transfers, possibly contributing to an over-subtraction at energy transfers below 0.2 meV. Notwithstanding these ambiguities we believe that this data provides a fair representation of the inelastic magnetic scattering in  $\{\text{Mo}_{72}\text{Fe}_{30}\}$ .

The magnetic nature of the observed spectrum was confirmed by studying the effect of an externally applied magnetic field. As illustrated by the base temperature data in Fig. 3 the application of a field leads to a noticeable broadening of the peak. With increasing magnetic field the intensity of the main peak near 0.6 meV decreases and the scattering distribution broadens. Examining the difference between scattering at zero and non-zero fields [14] shows that the spectrum in a field consists

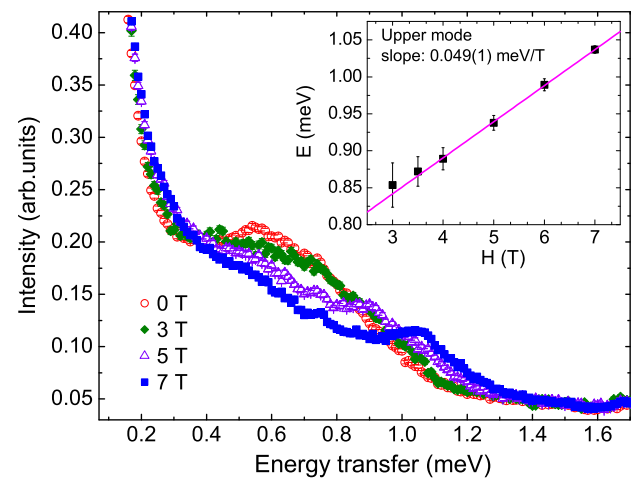


FIG. 3: Scattering at base temperature for several different values of applied magnetic field. Inset: Upper mode energy as a function of field.

of a central peak with two almost symmetric side bands, the positions of which vary roughly linearly with field strength. The position of the central peak shifts slightly with the applied field; the value at 7 T is estimated as  $0.50(1)$  meV. Following the detailed field dependence of the lower sideband quantitatively is difficult because of the large background at low energy transfers. The higher energy sideband can be observed more cleanly, and the peak position as a function of field is plotted in the inset to Fig. 3. For very small fields the side peaks cannot be resolved, but over the visible range the slope of the upper peak is  $0.049(1) \text{ meV/T}$ .

At present there is no rigorous theoretical calculation available for a detailed comparison with the results of this experiment. The large number of  $s = 5/2$  magnetic ions per molecule precludes the diagonalization of the quantum Heisenberg Hamiltonian. However, the main features of the energy spectrum can be established using a solvable effective 3-sublattice Hamiltonian [8, 10] as a starting point. Defining the total spin on each sublattice as  $\tilde{\mathbf{S}}_\alpha$  the Hamiltonian in the absence an external magnetic field is taken as  $\frac{J}{5} (\tilde{\mathbf{S}}_A \cdot \tilde{\mathbf{S}}_B + \tilde{\mathbf{S}}_B \cdot \tilde{\mathbf{S}}_C + \tilde{\mathbf{S}}_C \cdot \tilde{\mathbf{S}}_A)$ . This neglects anisotropy, which is estimated to be small compared to  $J$  [11]. The resulting spectrum has a hierarchy of discrete energy levels for each value of the total spin quantum number  $S$  given by  $E(S) = \frac{J}{10} (S(S+1) - S_A(S_A+1) - S_B(S_B+1) - S_C(S_C+1))$ , where the spin quantum numbers span the range  $0 \leq S \leq 75$  and  $0 \leq S_{A,B,C} \leq 25$ . The low-lying excitations form a sequence of well-separated, highly degenerate “rotational bands” with excitation energies depending quadratically on  $S$ . The energy levels in the lowest two rotational bands are given as  $E_1(S) = \frac{J}{10} S(S+1)$  and  $E_2(S) = 5J + E_1(S)$  with degeneracies for  $S \leq 50$   $D_1 = (2S+1)^2$  and  $D_2 = 27(2S+1)^2$ . The corresponding

levels of the exact Heisenberg model can be expected to differ by splittings of these levels.

Using the value of  $J = 1.57$  K found to describe the susceptibility data [9] and the selection rules  $\Delta S, \Delta M = 0, \pm 1$  for neutron scattering leads to an estimate of the gap between the the ground state and the first excited state within the band  $E_1(S)$  as  $J/5 \approx 27$   $\mu\text{eV}$ . The large elastic background precludes an observation of this mode in the present experiment. Using the same energy scale, transitions from the ground state to the second rotational band should produce a pronounced intensity near  $5J \approx 0.67$  meV, consistent with the broad band of excitations seen at base temperature, as shown in the inset to Fig. 1.

The detailed lineshape of the base temperature scattering may reflect the richer structure of the energy spectrum of the nearest-neighbor Heisenberg model, as compared to that of the rotational band model. It may also reflect the effects of weak anisotropy. A recent approximate spin-wave calculation [12] for the nearest-neighbor model with anisotropy predicts that several modes should be visible in the region of interest. A full understanding of the line shape requires further theoretical work.

The temperature dependence of the scattering as shown in Fig. 2 can also be considered within the context of the rotational band model. As the temperature increases above  $T \geq J/5 \approx 0.3$  K, energy levels within the lowest band become more populated, giving rise to the broadening and shifting of the main excitation towards  $E = 0$ . A detailed comparison with experiment requires an evaluation of matrix elements. A calculation was carried out starting from standard formulas for magnetic neutron scattering [15], using a common nonzero matrix element for all allowed transitions [16]. Thermal occupation of levels was accounted for by a Boltzmann factor, and Dirac delta function factors associated with allowed transitions were replaced by a Lorentzian with a width of 0.3 meV. The inset to Fig. 2 shows the resulting calculated curves using  $J = 1.57$  K. Despite the simplified nature of the approximations made there is a striking resemblance between the curves and the data. The peak position of the theoretical curve at 65 mK is in reasonable agreement with observations. For successively higher temperatures the peak broadens and shifts to lower energies. Near 7 K the peak in the intensity occurs at around 0.2 meV, similar to that seen experimentally. The simplified rotational band model provides a reasonable explanation for the qualitative behavior with temperature.

An extension of the rotational-band model to non-zero fields predicts that the ground state gradually shifts to  $S > 0$  states preserving the quadratic dependence on  $S$  in both the lowest and first rotational bands [10]. Zeeman splitting of the levels leads to excitations whose energies vary linearly with the magnetic field. However, a quantitative theoretical explanation of the field dependence of the neutron scattering cross-section remains as an open problem.

In summary, using inelastic neutron scattering we have measured the temperature and magnetic field dependence of magnetic excitations in the Keplerate molecular magnet  $\{\text{Mo}_{72}\text{Fe}_{30}\}$ . A solvable three-sublattice model [10] accounts for the overall energy scale and qualitative temperature dependence of the observed inelastic scattering. The principal mode observed can be understood as arising from transitions between the two lowest rotational bands. A quantitative understanding of the detailed  $T = 0$  lineshape and the behavior in a magnetic field will require a more sophisticated theory. We hope that these results will stimulate the continued development of theoretical methods incorporating the essential qualitative features and symmetries of the system, and that these will prove useful for other systems where diagonalization of the Hamiltonian cannot be performed. Finally we note that the neutron scattering experiments on large magnetic molecules are currently very difficult, nonetheless important new information is attainable now, and next generation instrumentation presents significant new opportunities.

The authors thank R. J. McQueeney and B. Normand for helpful discussions. Work at ORNL is supported by the U.S. DOE under Contract No. DE-AC05-00OR22725 with UT-Battelle, LLC and work at Ames Laboratory was supported under Contract No. W-7405-Eng-82. The work at NIST was supported in part by the NSF under Agreement No. DMR-0086210. The work at Universität Osnabrück was supported by DFG No. SCHN-615/5-2. The OSIRIS measurements (DAT, BL) were supported by UK EPSRC GR/N35038/01.

---

\* Electronic address: garlea@ornl.gov

- [1] See, e.g., J. Schnack in Lecture notes in Physics Vol. **645**, *Quantum Magnetism*, Springer, Berlin (2004).
- [2] M. Hennion *et al.*, Phys. Rev. B **56**, 8819 (1997).
- [3] Y. Zhong *et al.*, J. Appl. Phys., **85**, 5636 (1999).
- [4] G. Chaboussant *et al.*, Phys. Rev. B **70**, 104422 (2004).
- [5] R. Caciuffo *et al.*, Phys. Rev. Lett. **81**, 4744 (1998).
- [6] S. Carretta *et al.*, Phys. Rev. B **67**, 094405 (2003).
- [7] O. Waldmann *et al.*, Phys. Rev. Lett. **91**, 237202 (2003).
- [8] M. Axenovich and M. Luban, Phys. Rev. B **63**, 100407(R) (2001).
- [9] A. Müller *et al.*, ChemPhysChem. **2**, 517 (2001).
- [10] J. Schnack, M. Luban, and R. Modler, Europhys. Lett. **56**, 863 (2001).
- [11] M. Hasegawa and H. Shiba, J. Phys. Soc. Jpn **73**, 2543 (2004).
- [12] O. Cépas and T. Ziman, cond-matt/0412244.
- [13] C. Schröder *et al.*, Phys. Rev. Lett. **94**, 017205 (2005).
- [14] V. O. Garlea *et al.* (to be published).
- [15] See, e.g. V. F. Turchin, *Slow Neutrons*, Sivan Press, Jerusalem (translation), 1965, or S. W. Lovesey, *Theory of Neutron Scattering from Condensed Matter Volume 1*, Clarendon Press, 1984.
- [16] M. Exler, J. Schnack, and M. Luban (to be published).